Ion transport across transmembrane pores

Leontiadou, Hari; Mark, Alan E.; Marrink, Siewert-Jan

Published in:
Biophysical Journal

DOI:
10.1529/biophysj.106.101295

Publication date:
2007

Ion Transport across Transmembrane Pores

Hari Leontiadou,* Alan E. Mark,† and Siewert-Jan Marrink*
*Groningen Biomolecular Sciences and Biotechnology Institute, Zernike Institute for Advanced Materials, University of Groningen, Nijenborgh 4 9747 AG, Groningen, The Netherlands; and †School of Molecular and Microbial Sciences and the Institute for Molecular Biosciences, University of Queensland, Brisbane QLD 4072, Australia

ABSTRACT To study the pore-mediated transport of ionic species across a lipid membrane, a series of molecular dynamics simulations have been performed of a dipalmitoyl-phosphatidyl-choline bilayer containing a preformed water pore in the presence of sodium and chloride ions. It is found that the stability of the transient water pores is greatly reduced in the presence of the ions. Specifically, the binding of sodium cations at the lipid/water interface increases the pore line tension, resulting in a destabilization of the pore. However, the application of mechanical stress opposes this effect. The flux of ions through these mechanically stabilized pores has been analyzed. Simulations indicate that the transport of the ions through the pores depends strongly on the size of the water channel. In the presence of small pores (radius <1.5 nm) permeation is slow, with both sodium and chloride permeating at similar rates. In the case in which the pores are larger (radius >1.5 nm), a crossover is observed to a regime where the anion flux is greatly enhanced. Based on these observations, a mechanism for the basal membrane permeability of ions is discussed.

INTRODUCTION

In biological systems, specific channels and transporters mediate the electrophysiological characteristics of membranes by selectively allowing ions to permeate through the hydrophobic lipid matrix. However, there is strong evidence to suggest that the transmembrane potential is also influenced by the passive permeation of ions through biological membranes, especially in electrically active tissues (1). Although the electrical properties of lipid bilayers have been studied extensively, the exact mechanism by which ions passively translocate is not yet understood. It has been previously suggested that water pores, which appear in the membrane as metastable defects, can provide a pathway for the translocation of ions (2–4). In this way ions may maintain their hydration shell and at the same time diffuse rapidly through the hydrophobic region of the interior of the membrane (5). A simple elastic model that accounts for the behavior of pores in membranes (6) is given by

$$E(r) = 2\pi r\gamma - \pi r^2\Gamma. \quad (1)$$

Here E is the energy of a transmembrane water pore of radius r, γ is the pore line tension, and Γ the surface tension of the membrane. The stability of these water pores thus results from the interplay between surface and line tension. Beyond the so-called rupture tension, pores once formed grow continuously, unless the total membrane area is constrained. In this case the energy cost to compress the membrane places an upper bound on the size of the pore. A range of experimental techniques exists that can be used to probe the formation and evolution of pores in model membranes. These techniques, which alter the balance between the various energetic contributions, include electroporation (7), pipette aspiration (8–11), and osmotic swelling (12). Pores can also be stabilized by other biologically relevant means such as the addition of lipids that promote positive curvature (11) or by the addition of antimicrobial agents (12,13). Stabilized pores are of biological as well as technological interest due to their ability to transport molecules across the membrane. For instance, small pores formed by antimicrobial peptides destroy transmembrane ion gradients and can lead to cell death. On the other hand, large stable pores generated by electroporation can be used to facilitate DNA uptake by cells (14,15).

Various molecular simulation techniques can be used to model the experimentally observed and theoretically predicted behavior of transmembrane pores and provide a molecular picture of the formation and structure of these nanoscale pores in lipid membranes (16–25). Here we use the molecular dynamics (MD) simulation technique to study the permeation of ions through tension stabilized transmembrane pores. We have performed MD simulations of a DPPC (dipalmitoyl-phosphatidyl-choline) bilayer containing sodium chloride ions in a buffer at a range of ionic strengths (0 M, 0.1 M, 0.2 M, and 0.6 M). Both the transport of the ions through the pores and the effect of salt on the stability of such pores were examined. By combining the free energy profile of dissolving ions in the pore, their diffusion rate across the pore, and the relative stability of the pore, it has also been possible to estimate the pore-mediated permeation rates.

METHODS

Simulation setup

The model of the DPPC bilayer used in this study was similar to that used in a previous study of the stability of transient water pores in a pure DPPC lipid

Submitted November 17, 2006, and accepted for publication February 7, 2007.

Address reprint requests to Siewert-Jan Marrink, E-mail: s.j.marrink@rug.nl.

0006-3495/07/06/4209/07 $2.00

doi: 10.1529/biophysj.106.101295

bilayer (20). The water was described by the simple point charge (SPC) model (26). The parameters for the ions were taken from Straatsma and Berendsen (27). The system consisted of 128 DPPC lipids and 5909–6009 water molecules. The ionic strength was varied by adding an appropriate number of sodium and chloride ions. This was achieved by randomly substituting water molecules with sodium or chloride ions. In total 20 (0.1 M), 40 (0.2 M), and 120 (0.6 M) sodium and chloride atoms were inserted into the water phase. The MD simulations were performed using the GROMACS package, version 3.05 (28). Periodic boundary conditions were applied and the temperature was coupled to 323 K using a Berendsen thermostat (29). At this temperature the membrane is in the biologically relevant fluid phase. The long-range electrostatic interactions were evaluated using the particle mesh Ewald (PME) method. A 5-fs time step was used (30). Bond lengths were constrained using the LINCS algorithm (31). Two types of simulations were performed at constant surface pressure (N P_z $P_{\|}$ T) and at constant area (N P_z A T).

In all simulations the pressure in the direction normal to that of the plane of the membrane was weakly coupled to a pressure bath at 1 bar (29). For the simulations performed under constant surface pressure, the pressure in the lateral (*xy*) plane was varied between −10 bar to −50 bar, also using the weak coupling scheme. In this way a tension of ~9–30 mN/m was imposed on the surface of the bilayer. For the simulations at constant area the lateral dimensions of the box (*xy* plane) were kept constant. The simulations were performed starting from two different conformations. One was an equilibrated bilayer and the other was a bilayer with a preformed transient pore. Both systems were simulated with a range of different conditions applied to the membrane and at different ionic strengths of the solution (Table 1). Equilibration times of bilayers in the presence of ions are a point of concern. Simulations performed by Bockman et al. (32) revealed correlation times for the binding of sodium ions to lipids of the order of 50 ns. The slow equilibration times of the systems show up in the ion density profiles (not shown), which are not symmetric even after almost 100-ns simulation time.

Tension stabilized pores

In our previous work it has been shown that hydrophilic pores in a pure DPPC lipid bilayer can be stabilized by the application of membrane tension that is on the order of 9–18 mN/m. The application of tension increases slightly the size of the pores as well as increasing their lifetimes. By applying tension to the bilayer without any salt present, the pores could be maintained open during the simulations that had a time length ranging between 50 ns and 100 ns. These results were, however, obtained from simulations in which a 1.4-nm cutoff plus a reaction field correction was used to evaluate the long-range electrostatic interactions (33). To demonstrate that the current simulations would be consistent with the previous results, simulations of a pure DPPC bilayer were performed using the PME method to calculate the electrostatic interactions and compared with the results obtained previously. No significant differences were observed. Using tensions in the range of 9–15 mN/m, pores remained open for as long as 50 ns, the timescale of the simulations. To study the effect of salt on the stability of these transient pores, the water channels have been simulated under similar conditions to that described previously for a pure bilayer except for the use of PME and the inclusion of sodium chloride ions in the solutions.

TABLE 1 Overview of the simulations of a DPPC bilayer under different conditions

Label	Lateral pressure (−bar)	Surface tension (mN/m)	Ions (M)	Simulation time (ns)
Pure DPPC bilayer with a preformed pore				
A	10	9	0	79
B	20	15	0	46
C	30	19	0	31*
D	35	20	0	17*
DPPC bilayer with a preformed pore and NaCl ions				
E	10	9	0.1	75†, 39†, 20†
F	10	9	0.2	20†, 39†, 14†
G	20	16	0.2	10†
H	30	23	0.2	51
I	35	26	0.2	79
J	35	26	0.2	70
K	40	26	0.2	70
L	50	31	0.2	10*
M	10	9	0.6	7†, 8†, 8†
Equilibrated DPPC bilayer with NaCl ions				
N	1	0	0.1	22
O	1	0	0.2	65
Constant area simulation				
P	1	0	0.2	92

*Membrane ruptures.
†Pore closes.

Estimation of pore size

To estimate the size of the pore, the number of water molecules in the interior of the pore has been calculated. This was achieved by defining a region corresponding to the hydrophobic interior of the membrane. A region has been defined as a slice through the membrane extending 0.8 nm on either side of the center of the membrane. The number of water molecules in this region was counted and averaged over a periods of 1 ns. This provides a rough estimate of the time-dependent size of the water pore. It should be noted that using this approach the water molecules located at the openings of the pore were not counted. During the simulations performed at constant lateral pressure, it was found that the pore size during the simulations showed large fluctuations. For example, in simulations I and J the pore slowly expands over 20–50 ns. The large fluctuations observed in the tension-stabilized pores might in part be caused by the slow equilibration of the ions between the two monolayers. Consequently, the ions permeate a pore that varies in size over time. Therefore, to estimate the permeation rates for the sodium and chloride ions three types of pores have been distinguished. A small pore that contains ~100 water molecules, a medium size pore (~200 water molecules), and a large pore (>200 water molecules).

Free energy calculation

The free energy profile of the ions in the simulation box has been calculated using the following equation:

$$\Delta G = k_B T \ln(\rho_{aq}/\rho_z), \tag{2}$$

where k_B is the Boltzmann constant, T is the temperature, ρ_{aq} is the density of the ion in the central part of the water layer (assumed bulk-like), and ρ_z is the density of the ion as a function of the position in the z-direction normal to that of the lipid bilayer (with $z = 0$ in the middle of the bilayer).

Line tension

An important parameter that reflects the stability of the water pore is the line tension γ. From the radius of the pore r^* at the critical tension Γ^*, the line tension can be estimated using equation

$$\gamma = r^* \times \Gamma^*. \tag{3}$$

Ion flux

To investigate the flux of ions through the lipid bilayer, the mobility of the ions in the simulation box has been analyzed in all the simulations. A flux event has been defined as the diffusion of an ion from one boundary that is

the average position of phosphate groups in one layer to the other, through the pore region. The number of flux events divided by the total simulation time gave an estimate of the microscopic flux (j_i), which is a unidirectional flux of ions per time. To compare the fluxes between different sized pores the fluxes obtained have been normalized by the area of the pores. This flux is denoted j_i^* and is expressed per unit time, per unit area.

RESULTS AND DISCUSSION

Sodium adsorbed, chloride repelled from pore

Fig. 1 shows snapshots of three tension stabilized transmembrane pores in a DPPC bilayer. By varying the amount of tension, pores could be obtained with radii of ~0.8 nm, 1.2 nm, and 1.8 nm (see Methods). The smallest pore is the minimal pore size that is stable, i.e., lowering the tension further results in the closure of the pore. The water inside such a pore is tightly associated with the lipid headgroups that line the pore. If the tension is increased, the pore widens and the water within the central region of the pore has more bulk-like properties. The distribution of ions in each of the systems is very similar. The sodium ions show a strong tendency to bind to the membrane interface, with a peak in the distribution of sodium ions at the level of the phosphate groups. In sharp contrast, the chloride ions appear to be repelled by the interface and are predominantly located in the region of bulk water. This apparent formation of a double layer is in line with previous MD simulations of the interaction of ions with lipid membranes (34,35). It is generally believed that ions penetrate deep into the membrane-water interface and strongly affect the dynamical and structural properties of the bilayer (36,37). The preferential binding of sodium to the interface is maintained inside the pore. Visual inspection of Fig. 1 shows that sodium ions are present within the transmembrane pore for each of the three pore sizes.

Chloride, however, is only able to penetrate the larger pores. Electroporation experiments of lipid vesicles filled with 0.2 M NaCl also suggest that sodium ions interact strongly with the walls of the pore (38). The preferential binding of sodium ions inside the pore revealed in our simulations is further quantified in Fig. 2, which shows the effective free energy profile for solvating ions inside the transmembrane pore. Results are shown for an enlarged pore (radius ~3 nm) compared to a membrane without a pore being present. The free energy profiles are based on an evaluation of the density distribution of sodium and chloride ions at equilibrium (see Methods). In the absence of a pore in the bilayer the chloride ions interact only weakly with the interface. To enter the pore the chloride ions need to overcome an energetic barrier on the order of 3 kJ/mol near the lipid interface. In contrast the sodium ions are strongly attracted to the interface, but they must overcome a barrier of ~4 kJ/mol to cross the pore. For the smaller pores the statistics of the ion distributions inside the pore are becoming too limited to obtain quantitative meaningful free energy estimates. The qualitative features (i.e., a lower free energy of sodium ions inside the bilayer compared to chloride and an activation barrier for both ion types at the pore entrance) are preserved, however.

Anion/cation selectivity changes with pore size

Based on the distribution of ions inside the pore it might be expected that sodium, being attracted to the membrane-water interface, would permeate the pore at a higher rate compared to that of chloride. However, this is not necessarily the case. The dynamics of the system also plays a major role in determining the migration rates of ions. The rate at which ions cross the membrane can be readily calculated from the simulations although the statistical significance is limited for all but the largest pore studied. The results are summarized in Table 2. It was found that in the case of small pores almost no ions permeated the bilayer at the timescale of our simulations, except for a single sodium ion. With the statistical limitations in mind we therefore estimate $j*_{Na} \sim 0.005\,ns^{-1}nm^{-2}$ and $j*_{Cl^-} \sim 0.0\,ns^{-1}nm^{-2}$ across the small pore. For the medium sized pore both sodium and chloride ions were observed to permeate. The permeation rate of the sodium ions through the medium sized pore was similar to that of the small pore. However, in contrast to the small pore, chloride ions were able to cross the medium pore at a rate even larger than that of sodium: $j*_{Cl^-} \sim 0.02\,ns^{-1}nm^{-2}$. The chloride ion flux was significantly further enhanced in the case of the large pore $j*_{Cl^-} \sim 0.1\,ns^{-1}nm^{-2}$, whereas the sodium flux increased only slightly to $j*_{Na^+} \sim 0.01\,ns^{-1}nm^{-2}$. Thus, for the larger pore the chloride ion flux was an order of magnitude larger than that of the sodium ions. Upon increasing the pore size, we observe a reversal from cation to anion selectivity.

As already alluded to, the origin of this effect is related to the dynamics of the ions inside the pore. Fig. 3 shows

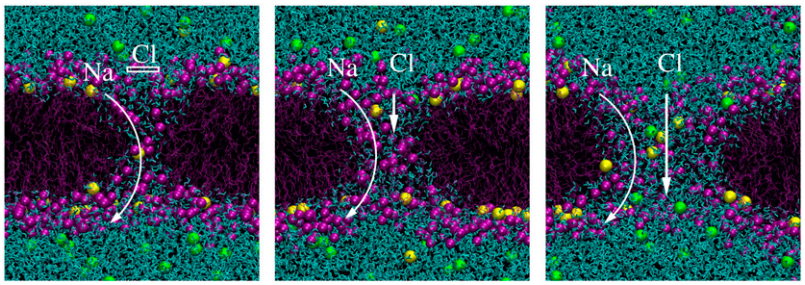

FIGURE 1 Snapshots of a small, a medium, and a large transmembrane pore observed in different simulations. Arrows indicate the path as well as the intensity of ion permeation through the pores. The water molecules are displayed as cyan sticks, phosphorus atoms in the lipid headgroups are mauve spheres, lipid tails are purple sticks, chloride anions are green spheres, and sodium cations are yellow spheres.

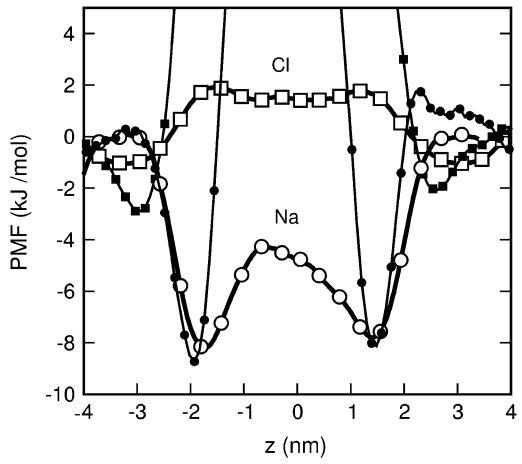

FIGURE 2 Potential of mean force (PMF) across a lipid bilayer for sodium (*circles*) and chloride (*squares*) ions. The PMFs of the ions have been calculated for an equilibrated bilayer without a pore, simulation O (*solid symbols*), and for a bilayer that contains a large pore, simulation K (*open symbols*). The middle of the bilayer corresponds to $z = 0$.

representative trajectories of both a sodium and a chloride ion inside the pore. The average time required for a chloride ion to pass through the pore was much shorter than for a sodium ion. The chloride ions spend an average of <1 ns inside the pore. In contrast the sodium ions require $\sim$10 ns to cross the pore. Note that these estimates reflect passage times across the largest pore. For narrower pores the passage times are presumably larger, explaining our observation of only a single sodium ion being able to cross the smallest pore in a total of 130-ns simulation time, despite the clear presence of sodium ions inside the pore (cf. Fig. 1). Although the interface attracts the sodium ions, it also restricts their motion. In contrast when the pore is of a sufficient size that the water within the pore is bulk-like, chloride may cross through the center of the pore at an overall rate that is higher than that of sodium. In Fig. 1 the permeation routes for the sodium and chloride ions across different sized pores are indicated schematically. Experimentally, anionic selectivity across lipid membranes has been reported for large pores stabilized by specific cationic lipids (39). The permeability ratio (P_{Cl}/P_K) of the ions through these pores is found to be $\sim$4–7. Another example of an anionic selective membrane pore is that formed by members of the magainin family of antimicrobial peptides. The pores formed by magainin peptides are estimated to be in the range of 2–3 nm and have a selectivity ratio of $P_{Cl}/P_K = 3$ (40,41). In both examples the pores are in principle large enough to contain bulk water. This said, it must also be noted that the composition of the membranes studied experimentally are quite different from the pure DPPC bilayer simulated in this work.

Permeation process of sodium/chloride

To relate the microscopic ion fluxes in the simulation to the macroscopic fluxes measured experimentally, the equilibrium density of pores inside the membrane must be estimated. The estimate we have is based on two assumptions. The first assumption is that small transient pores are formed due to spontaneous fluctuations in the lipid matrix and that this results in an equilibrium distribution of pores with a size similar to that of the minimal size obtained in our simulations. The second assumption is that the presence of ions does not affect this equilibrium pore density significantly. As we will show later, this second assumption only holds in the limit of low salt concentrations. Based on these assumptions, we will now proceed to establish a connection between the microscopic and the macroscopic permeation rates of ions across lipid membranes. Experimentally the equilibrium pore density is difficult to determine. However, based on recent detailed MD simulations of pore formation in a DPPC membrane (25,42) the free energy required to form a minimal sized pore has been estimated to be $\sim$80 kJ/mol. Assuming a Boltzmann weighted distribution, this corresponds to an equilibrium pore density of 18 pores per cm^2. Knowing the pore density, we can calculate the pore-mediated ion flux. The total flux of particle i through the membrane using pores is

$$J_i = j_i \rho, \tag{4}$$

where J_i is the total flux (particles per second per cm^2), j_i the flux through the pore (particles per second), and ρ the pore density (pores per cm^2). In the case of sodium ions the rate of permeation rate is not strongly dependent on the size of the pore (see Table 2). Thus although the statistics for the permeation of sodium through the small pore are limited, the value obtained is consistent in all the simulations. Using a value of $j_{Na} \sim 107$ s^{-1} we find a total flux of $J_{Na} \sim 2 \times 10^8$ particles cm^{-2} s^{-1}. From the flux we can estimate the permeability coefficients P, using

TABLE 2 Estimation of the permeation rates for the sodium and chloride ions

Pore type	Simulation	No. Na [ns^{-1}]	j_{Na} [ns^{-1}]	j^*_{Na} [ns^{-1}nm^{-2}]	No. Cl [ns^{-1}]	j_{Cl} [ns^{-1}]	j^*_{Cl} [ns^{-1}nm^{-2}]
Small ($\sim$100 H_2O) Area $\sim$2 nm^2	H	0/51	0	0	0/51	0	0
	I	1/79	0.01	0.005	0/79	0	0
Medium ($\sim$200 H_2O) Area $\sim$4 nm^2	J	1/50	0.02	0.005	4/50	0.08	0.02
	P	2/92	0.02	0.005	6/92	0.06	0.015
Large ($>$200 H_2O) Area $\sim$9 nm^2	K	7/70	0.1	0.01	57/70	0.8	0.09 $\pm$ 0.01*

*The error bars are given only for the large pore; the number of flux events in the other cases is too small to determine statistically meaningful error bars.

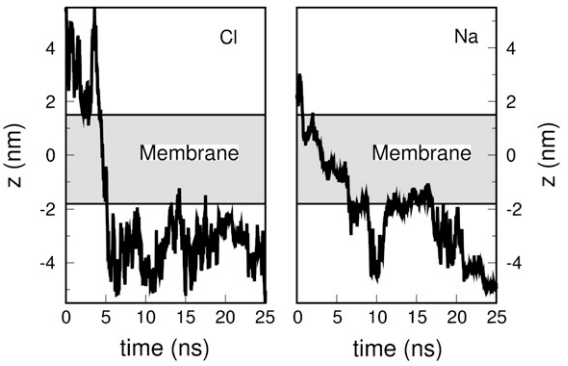

FIGURE 3 Plots of the coordinates of a typical example of one chloride (*left*) and one sodium (*right*) ion along the axis normal to that of the membrane as a function of time.

$$P_{\mathrm{i}} = \frac{J_{\mathrm{i}}}{\Delta C}, \tag{5}$$

where P is expressed in cm s^{-1} and ΔC denotes the difference in concentration driving the net transport of ions. Note that in the symmetric case there is no difference in concentration. Therefore, we estimate the permeability considering the unidirectional flux only. For sodium, with $\Delta C =$ 0.2 M, we find $P_{\mathrm{na}} = 1 \times 10^{-13}$ cm s^{-1}. This is comparable to the experimentally measured permeation rate of sodium through pure lipid bilayers of $P = 10^{-12} - 10^{-14}$ cm s^{-1} (43). Our results strongly suggest that sodium permeation occurs primarily through water pore defects. In the absence of pores, the ion flux is expected to be extremely low. Even if sodium ions were to retain their hydration shell, the free energy cost associated with the transfer of a sodium ion from water into the membrane interior is estimated to be of the order of 150 kJ/mol (44). In the case of chloride ions, the pore-mediated permeation rate predicted from the simulation is virtually zero, $J_{\mathrm{Cl}}, P_{\mathrm{Cl}} = 0$. Chloride ions were found to be unable to cross a pore of minimal size. In principle chloride ions could permeate the membrane via enlarged pores; however, in the absence of additional stabilizing factors the free energy cost associated with the formation of larger pores rapidly increases with pore size (25). Analysis of experimental data on the permeation rates of halide ions through phosphatidylcholine liposomes with different acyl chain lengths has shown that halide ion translocation occurs most likely via a mechanism in which the ions dissolve in and diffuse through the membrane directly and not via water pores (45). The simulations presented in this work provide an explanation for why chloride anions are unable to permeate small transient pores whereas sodium cations, by diffusing on the pore walls, are able to.

Line tension increases with salt

In the analysis of the macroscopic fluxes, it was assumed that the presence of ions does not have a significant influence on the probability to form a pore. This assumption is questionable and may only hold in the limit of low salt concentration. Evidence from experimental measurements (46) indicates that the propensity of the membrane to form pores diminishes with increasing ionic strength of the solution. On the other hand, recent simulations (23) have shown that the electric field produced by ions can, under certain conditions, be strong enough to induce spontaneous pore formation similar to electroporation. To resolve this apparent discrepancy we tested the effect of salt on the stability of the pores. Without ions, a pore can be effectively stabilized indefinitely (>100 ns) by a tension of 9 mN/m in the simulations. In the presence of ions, however, the quantitative behavior is changed (see Table 3). The apparent lifetime of the pore decreased as the concentration of ions was increased. Increasing the ion concentration from 0.1 M to 0.2 M results in the reduction of the lifetime of the pore from ~21 to 15 ns. Although the significance of this change could be debated, a further increase of the ion concentration to 0.6 M resulted in very rapid pore closure (~6 ns). The effect of ions is in line with the experimental evidence and can be interpreted as a salt-mediated increase of the line tension of the lipid bilayer.

From the results in Table 1 it is possible to estimate the critical tension of the bilayer with and without sodium chloride (0.2 M). The tension above which rupture of the membrane starts to occur in the pure bilayer is ~15 mN/m. However, in the presence of the sodium and chloride ions the critical tension increases to 23 mN/m, indicating that the stability of the bilayer has increased. The increase in line tension is calculated to be ~2-fold at 0.2 M. Whereas in a pure DPPC bilayer the line tension is estimated to be 1.5×10^{-11} N, in the presence of NaCl (0.2 M) this increases to $\sim 3 \times 10^{-11}$ N. In other words, the energy required to form the curved pore wall increases when ions are present. This can be understood as a consequence of the strong interaction of the sodium ions with the membrane-water interface, rendering the membrane stiffer. The increased stiffness of the membrane is also reflected by the decrease in equilibrium membrane area from 0.64 nm^2 for a DPPC bilayer in the absence of salt to 0.60 nm^2 at 0.2 M sodium chloride. These results are consistent with other recent simulation studies (34,35) as

TABLE 3 Dependence of the lifetime of the pore on the concentration of the ions

Ion concentration (M)	Simulation	Pore lifetime (ns)	⟨Pore lifetime⟩ (ns)
0.0	A	>79	>79
0.1	E1	10	21 ± 9
	E2	32	
	E3	20	
0.2	F1	10	15 ± 8
	F2	9	
	F3	26	
0.6	M1	6	6 ± 0.6
	M2	6.5	
	M3	5	

well as with experimental observations. The critical tension needed to rupture membrane vesicles has been measured (46) at varying ionic strengths in micropipette aspiration experiments. Increasing the ion concentration or the affinity of the ions to the lipids increases the critical tension of the membrane, thus making the membrane more stable.

General permeation process of ions

Finally we can speculate about the flux of other ions, such as proton, potassium, and calcium, through water pores similar to those present in our simulations. There is evidence to suggest that the permeation of potassium, as well as protons, occurs through transient water pores (47). The transport of protons through lipid bilayers is anomalously high compared to other cations. The permeability coefficient for protons is 3–5 orders of magnitude higher than that of sodium (47). Protons are able to propagate along thin water wires (24,48). A water pore of minimal size already satisfies such a criterion and would therefore allow for fast proton translocation. This small pore would also be sufficient for the sodium cations translocation. However, the sodium cations would diffuse much slower in the pore than the protons. The permeation rate of potassium is expected to be similar to that of sodium (on the order of 10^{-13} cm/s). Divalent calcium, however, binds to the interface even more strongly than sodium (49). As a result, diffusion across the pores is expected to be even slower than that of sodium. Moreover, binding of calcium ions at the interface would increase the line tension of the membrane, making pores less likely to form.

CONCLUSIONS

The MD simulations of ion transport across transmembrane pores suggest that the sodium and chloride ions permeate the water pores via different mechanisms. Whereas sodium is adsorbed to the membrane and diffuses across the interface, chloride prefers the bulk water in the middle of the pore. As a consequence, a crossover from cation-specific to anion-specific permeation is observed upon increasing the pore radius. For a pore of minimal radius, the simulations suggest that only sodium is able to permeate through the pore at a rate which can be compared to the basal permeation rate of sodium across lipid bilayers. For chloride ions this pore-mediated permeation route is only possible for pores that are enlarged through additional stabilizing factors. Furthermore we showed that an increase of the overall salt concentration has a destabilizing effect on the transmembrane pores, suggesting that the macroscopic permeation rates drop upon increasing ionic strength.

REFERENCES

1. Piguet, P., and R. A. North. 1992. The inward rectifier potassium conductance in rat basophilic leukemia cells. *J. Cell Phys.* 151:269–275.
2. Lawaczeck, R. 1988. Defect structures in membranes: routes for the permeation of small molecules. *Ber. Bunsenges. Phys. Chem.* 92: 961–963.
3. Jansen, M., and A. Blume. 1995. A comparative study of diffusive and osmotic water permeation across bilayers composed of phospholipids with different head groups and fatty acyl chains. *Biophys. J.* 68:997–1008.
4. Hamilton, R. T., and E. W. Kaler. 1990. Alkali metal ion transport through thin bilayers. *J. Phys. Chem.* 94:2560–2566.
5. Wilson, M. A., and A. Pohorille. 1996. Mechanism of unassisted ion transport across membrane bilayers. *J. Am. Chem. Soc.* 118:6580–6587.
6. Litster, J. D. 1975. Stability of lipid bilayers and red blood cell membranes. *Phys. Lett. A.* 53:193–194.
7. Melikov, K. C., V. A. Frolov, A. Shcherbakov, A. V. Samsonov, Y. A. Chizmadzhev, and V. Chernomordik. 2001. Voltage induced nonconductive pre-pores and meta-stable single pores in unmodified planar lipid bilayers. *Biophys. J.* 80:1829–1836.
8. Zhelev, D. V., and D. Needham. 1993. Tension-stabilized pores in giant vesicles: determination of pore size and pore line tension. *Biochim. Biophys. Acta.* 1147:89–104.
9. Olbrich, K., W. Rawicz, D. Needham, and E. Evans. 2000. Water permeability and mechanical strength of polyunsaturated lipid bilayers. *Biophys. J.* 79:321–327.
10. Sandre, O., L. Moreaux, and F. Brochard-Wyart. 1999. Dynamics of transient pores in stretched vesicles. *Proc. Natl. Acad. Sci. USA.* 96: 10591–10596.
11. Karatekin, E., O. Sandre, H. Guitouni, N. Borghi, P. Puech, and F. Brochard-Wyart. 2003. Cascades of transient pores in giant vesicles: line tension and transport. *Biophys. J.* 84:1734–1749.
12. Ludtke, S. J., K. He, W. T. Heller, T. A. Harroun, L. Yang, and H. W. Huang. 1996. Membrane pores induced by magainin. *Biochemistry.* 35:13723–13728.
13. Allende, D., S. A. Simon, and T. J. McIntosh. 2005. Melittin-induced bilayer leakage depends on lipid material properties: evidence for toroidal pores. *Biophys. J.* 88:1828–1837.
14. Smith, K. C., J. C. Neu, and W. Krassowska. 2004. Model for creation and evolution of stable electropores for DNA delivery. *Biophys. J.* 86:2813–2826.
15. Yoshizato, K., T. Nishi, T. Goto, S. B. Dev, H. Takeshima, T. Kino, K. Tada, T. Kimura, S. Shiraishi, M. Kochi, J. I. Kuratsu, G. A. Hofmann, and Y. Ushio. 2000. Gene delivery with optimized electroporation parameters shows potential for treatment of gliomas. *Int. J. Oncol.* 16:899–905.
16. Marrink, S. J., E. Lindahl, O. Edholm, and A. E. Mark. 2001. Simulation of the spontaneous aggregation of phospholipids into bilayers. *JACS.* 123:8638–8639.
17. Shillcock, J. C., and U. Seifert. 1998. Thermally induced proliferation of pores in a model fluid membrane. *Biophys. J.* 74:1754–1766.
18. Groot, R. D., and K. L. Rabone. 2001. Mesoscopic simulation of cell membrane damage, morphology change and rupture by nonionic surfactants. *Biophys. J.* 81:725–736.
19. Loison, C., M. Mareschal, and F. Schmid. 2004. Pores in bilayer membranes of amphiphilic molecules: coarse-grained molecular dynamics simulations compared with mesoscopic models. *J. Chem. Phys.* 121:1890–1900.
20. Leontiadou, H., A. E. Mark, and S. J. Marrink. 2004. Molecular dynamics simulations of hydrophilic pores in lipid bilayers. *Biophys. J.* 86:2156–2164.
21. Tolpekina, T. V., W. K. den Otter, and W. J. Briels. 2004. Nucleation free energy of pore formation in an amphiphilic bilayer studied by molecular dynamics simulations. *J. Chem. Phys.* 121:12060–12066.
22. Vernier, P. T., M. J. Ziegler, Y. Sun, W. V. Chang, M. A. Gundersen, and D. P. Tieleman. 2006. Nanopore formation and phosphatidylserine externalization in a phospholipid bilayer at high transmembrane potential. *J. Am. Chem. Soc.* 128:6288–6289.

23. Gurtovenko, A. A., and I. Vattulainen. 2005. Pore formation coupled to ion transport through lipid membranes as induced by transmembrane ionic charge imbalance: atomistic molecular dynamics study. *J. Am. Chem. Soc.* 127:17570–17571.

24. Tepper, H. L., and G. A. Voth. 2005. Protons may leak through pure lipid bilayers via a concerted mechanism. *Biophys. J.* 88:3095–3108.

25. Wohlert, J., W. K. den Otter, O. Edholm, and W. J. Briels. 2006. Free energy of a trans-membrane pore calculated form atomistic molecular dynamics simulations. *J. Chem. Phys.* 124:154905.

26. Berendsen, H. J. C., J. P. M. Postma, W. F. van Gunsteren, and J. Hermans. 1981. Interaction models for water in relation to protein hydration. *In* Intermolecular Forces. B. Pullman, editor. Reidel, Dordrecht, The Netherlands.

27. Straatsma, T. P., and H. J. C. Berendsen. 1988. Free energy of ionic hydration: analysis of a thermodynamic integration technique to evaluate free energy differences by molecular dynamics simulations. *J. Chem. Phys.* 89:5876–5886.

28. Lindahl, E., B. Hess, and D. van der Spoel. 2001. GROMACS 3.0: a package for molecular simulation and trajectory analysis. *J. Mol. Model. (Online).* 7:306–317.

29. Berendsen, H. J. C., J. P. M. Postma, W. F. van Gunsteren, A. Di Nola, and J. R. Haak. 1984. Molecular dynamics with coupling to an external bath. *J. Chem. Phys.* 81:3684–3690.

30. Feenstra, K. A., B. Hess, and H. J. C. Berendsen. 1999. Improving efficiency of large time-scale molecular dynamics simulations of hydrogen-rich systems. *J. Comp. Chem.* 20:786–798.

31. Hess, B., H. Bekker, H. J. C. Berendsen, and J. G. M. Fraaije. 1997. LINCS: a linear constraint solver for molecular simulations. *J. Comp. Chem.* 18:1463–1472.

32. Bockmann, R. A., A. Hac, T. Heimburg, and H. Grubmuller. 2003. Effect of sodium chloride on a lipid bilayer. *Biophys. J.* 85:1647–1655.

33. Tironi, I. G., R. Sperb, P. E. Smith, and W. F. van Gunsteren. 1995. A generalized reaction field method for molecular dynamics simulations. *J. Chem. Phys.* 102:5451–5459.

34. Pandit, S. A., D. Bostick, and M. L. Berkowitz. 2003. Molecular dynamics simulations of a dipalmitoylphosphatidylcholine bilayer with NaCl. *Biophys. J.* 84:3743–3750.

35. Mukhopadhyay, P., L. Monticelli, and D. P. Tieleman. 2004. Molecular dynamics simulation of a palmitoyl-oleoyl phosphatidylserine bilayer with Na+ counterions and NaCl. *Biophys. J.* 86:1601–1609.

36. Loshchilova, E., and B. Karvaly. 1978. Laser Raman studies of interaction in DPPC multilayers. Effect of mono and divalent ions. *BBA.* 514:274–285.

37. Binder, H., and O. Zschornig. 2002. The effect of metal cations on the phase behavior and hydration characteristics of phospholipid membranes. *Chem. Phys. Lipids.* 115:39–61.

38. Griese, T., S. Kakorin, and E. Neumann. 2002. Conductometric and electrooptic relaxation spectrometry of lipid vesicle electroporation at high fields. *Phys. Chem. Chem. Phys.* 4:1217–1227.

39. Chanturiya, A., J. Yang, P. Scaria, J. Stanek, J. Frei, H. Mett, and M. Woodle. 2003. New cationic lipids form channel-like pores in phospholipid bilayers. *Biophys. J.* 84:1750–1755.

40. Matsuzaki, K. 1998. Magainins as paradigm for the mode of action of pore forming polypeptides. *Biochim. Biophys. Acta.* 1376:391–400.

41. Duclohier, H., G. Molle, and G. Spach. 1989. Antimicrobial peptide magainin I from Xenopus skin forms anion-permeable channels in planar lipid bilayers. *Biophys. J.* 56:1017–1021.

42. Tieleman, D. P., and S. J. Marrink. 2006. Lipids out of equilibrium: energetics of desorption and pore mediated flip-flop. *J. Am. Chem. Soc.* 128:12462–12467.

43. Deamer, D. W., and J. Bramhall. 1986. Permeability of lipid bilayers to water and ionic solutes. *Chem. Phys. Lipids.* 40:167–188.

44. Neumann, E., S. Kakorin, and K. Toensing. 1999. Fundamentals of electroporative delivery of drugs and genes. *Bioelectrochem. Bioenerg.* 48:3–16.

45. Paula, S., A. G. Volkov, and D. W. Deamer. 1998. Permeation of halide anions through phospholipid bilayers occurs by the solubility-diffusion mechanism. *Biophys. J.* 74:319–327.

46. Shoemaker, S. D., and T. K. Vanderlick. 2002. Intramembrane electrostatic interactions destabilize lipid vesicles. *Biophys. J.* 83:2007–2014.

47. Paula, S., A. G. Volkov, A. N. Van Hoek, T. H. Haines, and D. W. Deamer. 1996. Permeation of protons, potassium ions, and small polar molecules through phospholipid bilayers as a function of membrane thickness. *Biophys. J.* 70:339–348.

48. Krishnamoorthy, I., and G. Krishnamoorthy. 2001. Probing the link between proton transport and water content in lipid membranes. *J. Phys. Chem. B.* 105:1484–1488.

49. Bockmann, R. A., and H. Grubmuller. 2004. Multistep binding of divalent cations to phospholipid bilayers: a molecular dynamics study. *Angew. Chem. Int. Ed. Engl.* 43:1021–1024.